V. Nedovic and R. Willaert (Eds.), *Cell Immobilization Biotechnology*. Kluwer Academic Publ, Part II, Chapter 6, 411-423.

GROWTH OF INSECT AND PLANT CELLS IMMOBILIZED USING ELECTRIFIED LIQUID JETS

MATTHEUS F. A. GOOSEN
Department of Bioresource and Agricultural Engineering,
College of Agricultural and Marine Sciences,
Sultan Qaboos University P.O. Box 34,
Al-Khod 123, Muscat, Sultanate of Oman
Fax No. (968) 513-418 Email: theog@squ.edu.om

1. Introduction

In many bio-processing laboratories, major focus has been placed on attempting to find cell culture methods which can increase the concentration of cells and cell products and permit cost-effective large-scale production. Methods of animal cell culture have been developed (mainly for mammalian cells) and involve the use of hollow fibers, gel entrapment, ceramic cartridges and microcarriers [1]. It is generally recognized that compared to microbial systems, large-scale mammalian cell suspension culture has been limited, to some extent, by relatively low cell densities. The concentration of extracellular proteins such as monoclonal antibodies and growth factors produced by this method is low and purification from growth media is difficult. The same problems are also encountered in insect culture. Inlow and co-workers [2], for example, reported maximum insect cell densities of 5.5 x 10^6 cells/mL in a spinner flask. Hink [3], working with *T. ni* cells, obtained maximum polyhedra (AcNPV) concentrations of ca. 2.2 x 10^8 polyhedra/mL medium at a cell density of 3.8 x 10^6 cells/mL medium (i.e. ca. 60 polyhedra/cell). Knudson and Tinsley [4], using *S. frugiperda* cells, reported 12-40 polyhedra (150-500 IFU)/cell.

Microencapsulation, an alternative cell immobilization technique originally developed for use as an artificial pancreas for the treatment of diabetes, has been employed industrially for the enhanced production and recovery of high-value biologicals from animal cells. The encapsulation technique entraps viable cells within semipermeable polysaccharide-polycation microcapsules [for example, alginate/poly-L-lysine (PLL)]. The capsule membrane selectively

allows small molecules such as nutrients and oxygen to freely diffuse through, but prevents the passage of large molecules and cells. Posillico [5] reported the use of microencapsulation for the commercial production of monoclonal antibodies. However, while cell densities of ca. 1 x 10^8 cells/mL capsules were obtained after three weeks of culture, they reported that the cells appeared to grow preferentially near the interior surface of microcapsule membrane and speculated that this could have been due to mass transfer limitations during culture and/or to the presence of a viscous intracapsular alginate solution.

The first step in the making of a microcapsule is droplet formation. Let us consider one technique, electrostatic droplet generation (i.e. electrified liquid jet), which has become the primary method used in our laboratory.

2. Droplet Generation Using an Electrified Liquid Jet

Electrified liquid jets (i.e. electrostatic atomisation) and electrostatically assisted atomization have been employed in a variety of areas, including paint spraying [6], electrostatic printing [7], and cell immobilization [1, 8]. Recently, micro and nano capsules as small as 0.15 micrometers, for example, have been produced using 0.7 mm ID needles [9]. The effect of electrostatic forces on mechanically atomized liquid droplets was first studied in detail by Lord Rayleigh [10, 11] who investigated the hydrodynamic stability of a jet of liquid with and without an applied electric field.

When a liquid is subjected to an electric field, a charge is induced on the surface of the liquid. Mutual charge repulsion results in an outwardly directed force. Under suitable conditions, for example, extrusion of a liquid through a needle, the electrostatic pressure at the surface forces the liquid drop into a cone shape. Surplus charge is ejected by the emission of charged droplets from the tip of the liquid. The emission process depends on such factors as the needle diameter, distance from the collecting solution, and applied voltage (strength of electrostatic field [12]. Under most circumstances, the electrical spraying process is random and irregular, resulting in drops of varying size and charge that are emitted from the capillary tip over a wide range of angles. However, when the electrostatic generator configuration has been adjusted for liquid pressure, applied voltage, electrode spacing and charge polarity, the spraying process can become quite regular and periodic.

2.1 PRODUCTION OF ALGINATE BEADS USING ELECTRIFIED LIQUID JETS

The section starts with a detailed experimental description of electrostatic droplet generation for those not familiar with the technique [12] (Fig. 1). Attach a syringe pump to a vertical stand. Use a 10 mL plastic syringe and 22- or 26- gage stainless steel needles. A variable high voltage power supply (0-30 kV) with low current (less than 0.4 mA) is required. We have used a commercial power supply model 230-30R from Bertan (Hicksville, NY). Prepare 1.5% (w/v) $CaCl_2$ in saline (0.85 g NaCl in 100 mL distilled water). Saline can be replaced with distilled water if an alginate solution without cells is being extruded. Place the $CaCl_2$ solution in a petri dish on top of an adjustable stand. The

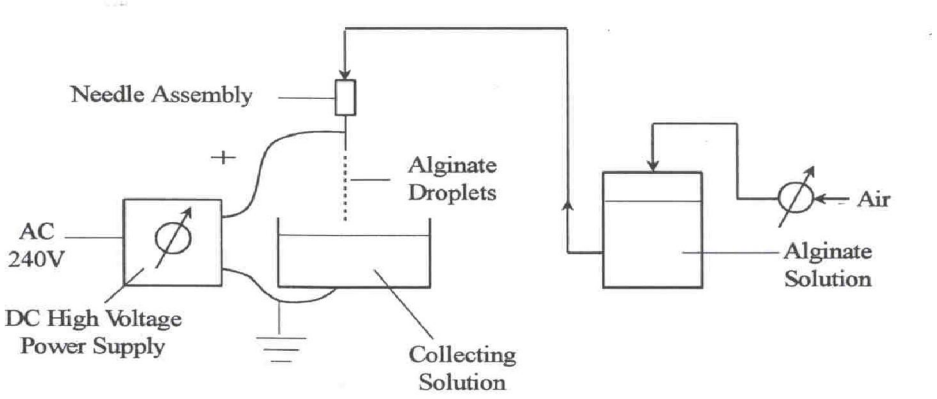

Figure 1. Electrostatic Droplet Generator System [18].

stand allows for fine tuning of the distance between the needle tip and collecting solution. Prepare 1 to 4 % (w/v) low viscosity sodium alginate by dissolving alginate powder with stirring in a warm water bath. Slowly add the 1 to 4 g sodium alginate to 100 mL warm saline solution (or distilled water), stirring continuously. It may take several hours to dissolve all of the alginate. Add about 8 mL of the alginate solution to a 10-mL plastic syringe, put back the plunger, and attach the syringe to the upright syringe pump. Make sure that the stainless steel needle, 22 gage, is firmly attached and the syringe plunger is in firm contact with the moveable bar on the pump. Position the petri dish (or beaker) containing $CaCl_2$ so that the needle tip is about 3 cm from the top of the $CaCl_2$ hardening solution. This is the primary reason for using an adjustable stand.

Attach the positive electrode wire to the stainless steel needle and the ground wire to the collecting solution. The wires may need some additional support to prevent them from bending the needle. Switch on the syringe pump and wait for the first few drops to come out of the end of the needle. This could take a minute or two. Doing it this way also ensures that the needle is not plugged. After the first drop or two has been produced, switch on the voltage supply. Make sure that the voltage is set low, less than 5 kV. If this is the first time that you have tried electrostatic droplet generation, raise the voltage slowly and observe what happens to the droplets. The rate at which they are removed from the needle tip increases until only a fine stream of droplets can be seen. The changeover from individual droplets to a fine stream can be quite dramatic. The most effective electrode and charge arrangement for producing small droplets is a positively charged needle and a grounded plate. Two other arrangements are also possible; positively charged plate attached to needle, and a positively charged collecting solution. Make sure that the positive charge is always on the needle. This ensures that the smallest microbead size is produced at the lowest applied potential. With a 22-gage needle and an electrode spacing of 2.5-4.8 cm there will be a sharp drop in microbead size at about 6 kV. This can be noticed visually by observing the droplets coming from the needle tip. Standard commercially available stainless steel needles can be employed. However, when going from a 22- to 26-gage (or higher) needle, needle oscillation may be observed. This needle vibration

will produce a bimodal bead size distribution with one peak around 50 µm diameter beads and another around 200 µm.

If a syringe pump is not available, remove the syringe plunger and attach an air line with a regulator to the end of the syringe. Varying the air pressure on the regulator can control the alginate extrusion rate.

Lumps of sodium alginate often form if the powder is added all at once to the warm saline. Sprinkle the alginate powder into the saline a small amount at a time with gentle mixing. Once it has dissolved (up to 1-2 h), allow the viscous solution to cool and then transfer it to several plastic test tubes, cap and store in the refrigerator until needed. This prevents bacterial growth. If the alginate solution is very viscous, air bubbles will be trapped during the stirring. These bubbles will disappear if the viscous solution is left to stand overnight.

If the needle is plugged, place it in dilute citrate solution for a few minutes. Passing a fine wire through the needle also helps. Resuspending cells in 1 % (w/v) sodium alginate solution will dilute the alginate and could give tear-drop shaped beads when the solution is extruded. To solve this problem, increase the concentration of sodium alginate solution to 3 or 4 %.

Extrusion of alginate droplets using a 5.7 KV fixed-voltage power supply showed that there is a direct relationship between the electrode distance and the bead diameter. For example, at 10-cm electrode distance, the bead diameter was 1500 µm while at 2 cm it decreased to 800 µm. The greatest effect on bead diameter was observed between 2 and 6 cm electrode distance. While there was overlap in bead sizes between 6, 8 and 10 cm electrode distance, there was a significant difference (i.e., no overlap in SD) between bead sizes at 2 and 6-cm electrode distance. An inverse relationship between needle size and microbead diameter was observed. Aside from the 23 G needle there was a significant difference between bead sizes produced by all needles (i.e., no SD overlap). As the needle size decreased from 19 to 26 G, the bead size decreased from 1400 to 400 µm, respectively. These results support previous work reported by Bugarski et al. (21). The present investigation showed that the alginate concentration does not appear to be important due to overlapping SD intervals for all data points. The bead diameter was found to be 800 µm at both 1% and 3 % alginate concentration.

Looking more closely at the effect of electrode distance on bead diameter, as a function of applied potential (Figure 2) we see that the decrease in microbead size was greatest between 5 and 10 KV for all electrode distances tested. The smallest bead, 200 µm, was produced at an electrode distance of 4 cm and an applied potential of 10 KV.

2.2 EFFECT OF ELECTROSTATIC FIELD ON CELL VIABILITY

To assess the effect of an electrostatic field on animal cell viability, an insect cell suspension was extruded using the electrostatic droplet generator. No detectable change in insect cell viability was observed after extrusion. The initial cell density, 4×10^5 cell/mL,

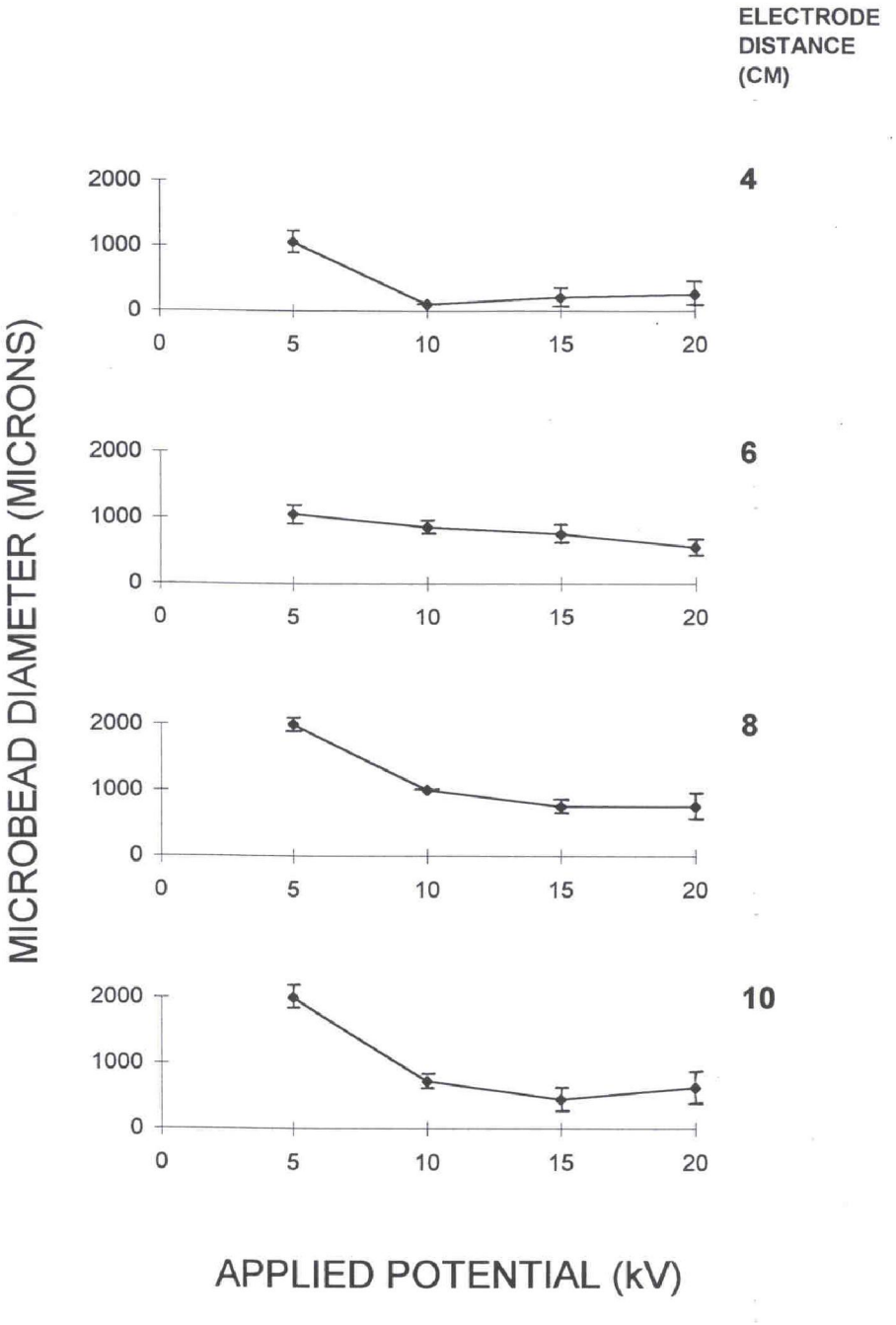

Figure 2. Effect of Electrode Distance and Applied Potential on Microbead Diameter [20].

remained essentially unchanged at 3.85 x 10^5 and 3.8 x 10^5 cell/mL immediately after passing through the generator at an applied potential difference of 6 and 8 kV, respectively. Prolonged cultivation of these cells did not show any loss of cell density or viability.

2.3 FORCES ACTING ON DROPLET IN AN ELECTRIC FIELD

In the absence of an applied voltage, a liquid drop falls from the end of a capillary tube at a critical drop volume dependent on the surface tension (i.e., the liquid drop would continue to grow until its mass overcomes the surface tension). If gravity were the only force acting on the meniscus of the droplet, large uniformly sized droplets would be produced with a radius r. Equating the gravitational force on the droplet to the capillary surface force gives:

$$r = (3 r_0 \gamma / 2 \rho g)^{1/3} \quad (1)$$

where r_o is the internal radius of the needle, γ is the surface tension, ρ is the relative density of the polymer solution and g is the acceleration constant.

Under the action of an electric field, the electric force, F_e, acting along with the gravitational force, F_g , would reduce the critical volume for drop detachment resulting in a smaller droplet diameter. Equating the gravitational and electrical forces on the droplet to the capillary surface force yields:

$$F_\gamma = F_g + F_e \quad (2)$$

Three electrode geometries were considered:

- A parallel plate arrangement in which the charge was applied to a plate held parallel to the collecting solution and through the centre of which the needle protruded (Figure 3A)
- Having the needle alone with the charge applied directly to the collecting solution (Figure 3B)
- Applying the charge to a solitary needle (Figure 3C).

In the case of a parallel plate electrode set up (Figure 3A) the electrostatic force exerted on a needle was found by modifying the expression obtained by Taylor [9, 13]:

$$F_e = \pi \varepsilon_o V^2 L^2 / H^2 [\ln(2L/r_0) - 3/2] \quad (3)$$

in which L is the height of the needle in the electric field, H is the electrode distance, V is the applied voltage, and ε_o is the permittivity of the air.

In the case of a charged needle (Figure 3C), the stress produced by the external field at the needle tip is obtained using a modified expression developed by DeShon and Carlson [14]:

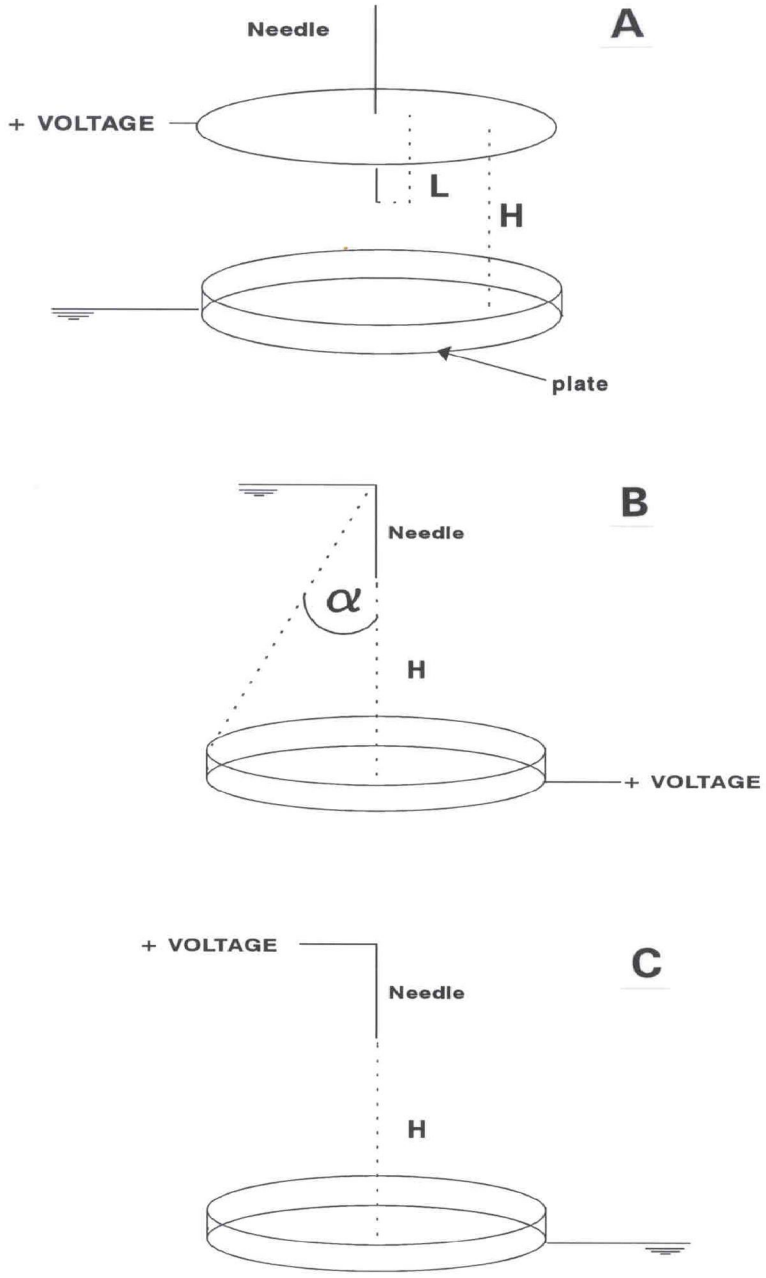

Figure 3. Electrode and charge arrangements; A: Parallel plate set-up with positively charged plate; B: Positively charged collecting plate; C: Positively charged needle[12, 26].

$$F_e = 4\pi \varepsilon_o V^2 / [\ln(4H/r_0)]^2 \quad (4)$$

Substituting Equation (3) into Equation (2) results in a relationship describing the effect of the applied potential on the droplet radius for the parallel plate arrangement:

$$r = \left([3/4\rho g] \left[r_o\gamma - (\varepsilon_o V^2 L^2) / \left(H^2 [\ln(2L/r_o) - 3/2] \right) \right] \right)^{1/3} \quad (5)$$

Similarly, the effect of applied potential on the droplet radius for the charged needle arrangement can be derived by substituting Equation (4) into (2):

$$r = \left([3/2\rho g] \left[r_o\gamma - (2\varepsilon_o V^2) / (\ln(4H/r_o)) \right] \right)^{1/3} \quad (6)$$

For the positively charged collecting plate and grounded needle (Figure 5B) an empirical relationship was obtained from the expression given by Hommel et al. [15]:

$$r = \left\{ [3/2\rho g] \left[r_o\gamma - (\varepsilon_o V^2 4\cos(\alpha)) / H \right] \right\}^{1/3} \quad (7)$$

in which α is the angle defined in Figure 3B.

The last three equations can be used to calculate the droplet size as a function of applied voltage for the three electrode geometries studied.

A comparison was made between the measured and calculated droplet/microbead diameters. The general shapes of the calculated curves were similar to those of the experimental curves. Very good agreement between experimental and calculated data was achieved with the 22 gauge needle in all three charge configurations. The calculated droplet diameter, for the range of applied potentials studied (2-12 kV), agreed well with the experimental data with an error of ± 15 %. Equally successful was the agreement for the 26 gauge needle, where the calculated and experimental data agreed within an error of ± 10 %.

As the voltage increased beyond a critical point (known as the minimum spraying potential), a transition from the dripping mode, where individual droplets could be seen to come off the end of the needle, to a high frequency spraying mode (i.e. liquid jet) was observed with all three charge arrangements. The minimum spraying potential for the positively charged needle set-up was observed to be lower than that for the parallel and charged plates. The process of droplet formation suggests that the forces due to the presence of an external electric field and the surface charge are responsible for the instability of the droplets at the needle tip. The charges which are distributed on the liquid surface repel each other and cause a force opposing the surface tension. In the case of the positively charged needle, the conducting liquid and needle are in close contact bearing approximately the same potential difference [16]. The electric field (E) at the meniscus is therefore proportional to the applied voltage, V , and radius of the meniscus, r_o. The area over which the surface charge operates varies with $1/r^2$. Due to

the small area available for charge distribution (the needle tip) the overall surface charge would be higher for this electrode arrangement, than for the two other set-ups at the same potential difference. For the parallel plate set-up, the uniform electric field between the two electrodes was proportional to the potential difference and electrode spacing, H. Therefore, a much higher potential difference was required to build a sufficiently large charge on the plate to initiate spraying (i.e. 8 kV for the parallel plate versus 5 kV for the positive needle set-up).

The positively charged plate, with grounded needle, is the reverse arrangement of the positively charged needle. Results with this geometry show that the reversed polarity had an impact on bead size with the charged plate set-up giving smaller bead sizes. This may be due to the larger area over which the surface charge has to spread, (i.e. the area of the hardening solution, $CaCl_2$). In this situation the charge density on the forming drop would be lower than in case of a positively charged needle, where the charge area was limited to the liquid meniscus at the needle tip. The net effect being a weaker force pulling the droplet from the tip of the needle.

3. Culture of Encapsulated Insect Cells

Insect cell culture has received an increased amount of attention recently since these cells are hosts for a class of viruses, the baculoviruses, which has been shown to be an excellent vector for genetic engineering, Luckow and Summers [17]. This is largely due to the high expression rate and post-translation processing capabilities of the baculovirus. Such processing includes efficient secretion, proteolytic cleaving, phosphorylation, N-glycosylation, and possibly myristylation and palmitylation.

The main objective of a study by King et al. [18], was to investigate whether insect cells (*Spodoptera frugiperda*) infected with a temperature-sensitive mutant of the *Autographa californica* Nuclear Polyhedrosis Virus (AcNPV ts-10) could be cultured to a high cell density in alginate/PLL microcapsules and whether the virus could be successfully grown and concentrated within the capsules. Ultimately, nonvirus genes were to be inserted into the temperature-sensitive virus in order to measure their expression and concentration in the microcapsule system.

3.1 GROWTH OF CELLS AND VIRUS IN MICROCAPSULES

The single- and multiple-membrane capsules produced using an initial alginate concentration of 1.4% were spherical in shape and showed no surface irregularities. The cells in the single-membrane capsules remained dispersed throughout the volume of the capsule and, after two days in culture, became enlarged and dark in color. Recovery of some of the cells from these capsules and subsequent staining with trypan blue indicated that few cells were living. In contrast, the cells in the multiple membrane capsules tended
to settle to the bottom of the capsule, indicating that the viscosity of the intracapsular solution was lower. After two days in culture, these cells appeared to be healthy (supported by trypan staining) although little sign of growth could be seen. The doubling time of insect cells is between 17 and 24 h.

The capsules which were produced using a 0.7% alginate/TC100/cell mixture were

nonspherical in shape and tended to have pointed ends, tails and creased sides. This non-sphericity, due to the low alginate concentration and hence low viscosity was most prevalent when the alginate concentration was 0.5% and was significantly reduced when increased to 0.6% or 0.7%. The capsules produced with a single, high-molecular-weight cutoff membrane (and either 0.7% or 1.4% alginate) tended to have weak membranes which broke easily and, consequently, allowed the cells within to escape and proliferate in the growth medium. In those few capsules which did not rupture, the infected cells grew in isolated clumps on the inside surface of the membrane. Intracapsular cell densities and virus titres were not measured in these capsules.

The capsules that possessed a multiple membrane (initial alginate concentration 0.7%) were much stronger and more flexible than their single-membrane counterparts as judged by pinching the capsules with fine tipped forceps. Consequently, there were fewer ruptured or broken capsules and significantly reduced numbers of cells were found in the supernatant. Cells grew and virtually filled the microcapsules (Figure 4) reaching maximum densities of 8×10^7 cells/mL. In comparison, maximum suspension culture densities were at least 10 times lower. The specific growth rate of encapsulated cells was 0.55 day^{-1}, and was comparable (though slightly lower) to the specific cell growth rates in shaker flasks, 0.66 day^{-1}, and monolayer culture, 0.78 day^{-1} (Table I).

The $TCID_{50}$ assay revealed that the titre of virus (ts10) in the capsules reached ca.1 x 10^9 infectious units (IFU)/mL (ca. 20 IFU/cell) and that of the supernatant was lower by a factor of 300. This indicates that virtually all of the virus (more than 99%) was retained within the capsules.

Table I. Comparison of growth rates of encapsulated and suspended insect cells [18].

Culture system	Specific growth rate (day^{-1})	Doubling time (h)
Suspended cells		
Shaker flasks	0.66	25
Monolayer (T-flasks)	0.78	21
Immobilized cells		
Microcapsules	0.55	30

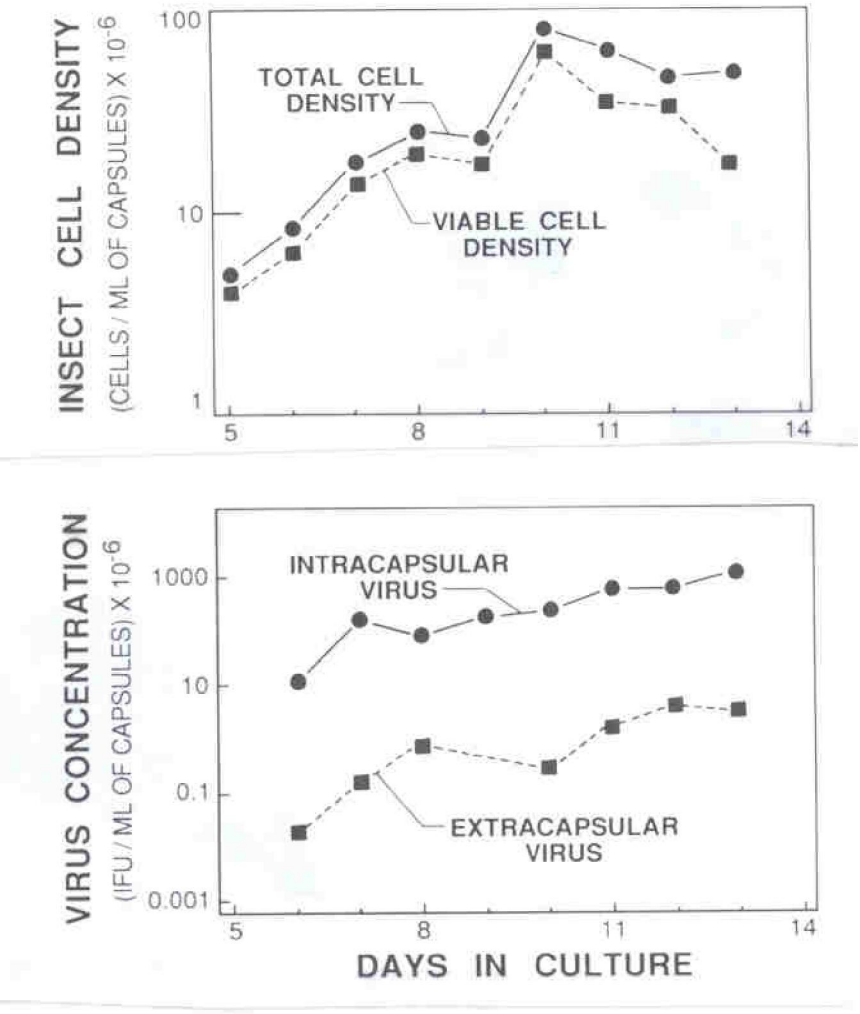

Figure 4. A. Intracapsular insect cell density as a function of time. Batch culture consists of 1-mL capsules in 30 mL medium; B. Intracapsular and extracapsular virus concentration as a function of culture time. At day 5, the culture temperature was dropped from 33 to 27°C to initiate virus growth in the infected insect cells[18].

Table II. Biocompatibility tests: Cells suspended in calcium alginate[18].

Alginate concentration	Cell viability
1.5% (w/v)	All cells enlarged, and dark most dead
1.3% (w/v)	All cells enlarged, and dark most dead
1.0% (w/v)	Some cells dark and granular while some are round and healthy; some cells have multiplied to form small masses
0.75% (w/v)	Good cell growth many cell masses
0.50% (w/v)	Good cell growth many cell masses

3.2 BIOCOMPATIBILITY OF ENACAPSULATION SOLUTIONS

The KCl, CHES, $CaCl_2$ and citrate solutions had no apparent effect on the growth of the cells. However, while exposure of the cells to PLL of $\bar{M}_v = 2.2 \times 10^4$ resulted in virtually no loss of cell viability, the cells exposed to PLL of $\bar{M}_v = 2.7 \times 10^5$ showed a 76% loss of viability. Cells exposed to alginate solutions showed a decrease in viability, which was dependent on the alginate concentration. On mixing the 2X TC100 and the alginate solutions, a gel-like material was produced, due, presumably, to the interaction between the calcium ions in the 2X TC100 (2.64 g/L) and the alginate. The gel tended to be more solid when the alginate concentration was 1.5%, 1.3%, and 1.0%, and was more liquid at 0.75% and 0.5% alginate. Cells suspended in mixtures of sodium alginate and TC100 [final concentrations of 1.5%, 1.3%, and 1.0% (w/v)] showed little or no growth and usually appeared dark and granular after 2-3 days (Table II). Trypan blue staining indicated that few if any cells were viable. Cell growth, however, was observed in the lower alginate/ TC100 mixtures [concentrations of 0.75% and 0.5% (w/v)].

Insect cells could not be cultured in either single- or multiple-membrane capsules when the initial intracapsular alginate concentration was 1.4%. The biocompatibility tests (Table II) support these results. Only at alginate concentrations of 0.75% or less was cell growth observed. In the biocompatibility tests cell density could not be measured directly since the cells were immobilized in calcium alginate gel. It can be postulated that the mechanism of cell growth inhibition may involve electrostatic interaction and/or viscosity effects between alginate and cells.

Cells encapsulated using single membrane capsules (molecular-weight cutoff of ca. 6×10^4) grew poorly. In this case, the membrane was relatively impermeable and, thus, only a small fraction of the alginate, with molecular weight of 3.5×10^5, could diffuse through. Cells encapsulated in single membrane capsules (molecular-weight cutoff of ca. 3×10^5) grew much better (though in isolated clumps) presumably because there was increased mass transfer and because more of the intracapsular alginate could diffuse out. Similar clumped cell growth has

been observed by other workers [5], who cultured hybridoma cells in single membrane microcapsules. The capsule membrane was also weak, causing some of the capsules to collapse and break, allowing the cells to escape into the medium. The capsule membrane molecular-weight cutoff was determined by incubating microcapsules (without cells) in solutions containing a protein standard. The protein concentration in the extracapsular (supernatant) solution was monitored and the membrane was deemed impermeable to the protein if there was 100% rejection of the diffusing protein over a two-hour period.

Multiple-membrane capsules, on the other hand, were significantly stronger than their single-membrane counterparts. Better cell growth was obtained with the former capsules, presumably due to the lower intracapsular alginate content. Why similar cell growth is not obtained in the high-molecular-weight, single-membrane capsules as occurs in the multiple-membrane capsules, is not clear since the intracapsular environment (i.e. viscosity) is believed to be virtually identical in both capsule types. One may postulate that the second PLL reaction in the multiple membrane procedure may further reduce the intracapsular alginate concentration in the bulk of the capsule by reacting with the alginate chains near the inside surface of the membrane. It is also unclear whether we have two distinct alginate/PLL membranes or one interacting membrane. The term multiple membrane refers more to the method of capsule preparation rather than to the type of final membrane.

When insect cells were exposed, for one minute, to PLL (0.05% with $\bar{M}_v = 2.7 \times 10^5$), 76% were killed. In contrast, cells exposed to PLL ($\bar{M}_v = 2.2 \times 10^4$) (0.05%) for one minute remained 100% viable. It was possible that some fraction of the PLL may have bound to the glass beaker in which the PLL was dissolved rather than remaining in solution thus lowering the bulk PLL concentration, or perhaps PLLs of different molecular weight may bind to the cells differently.

The ability to control virus replication by lowering the culture temperature has allowed the growth and concentration of virus inside of cell-filled microcapsules. Comparison of the number of IFU per cell obtained in the present study (ca. 20 IFU/cell) to that obtained by Knudson and Tinsley [4] (150-500 IFU/cell) suggests that our system is operating far below its optimum. Based on the data of Knudson and Tinsley, intracapsular virus concentrations should, when optimized, be approaching 2.5×10^{10} IFU/mL capsules.

4. Encapsulation and Growth of Plant Tissue in Alginate

Animal cell suspensions were successfully extruded using the electrostatic droplet generator. The application of this technology to plant cell immobilization has only recently been reported [19-21]. A major concern in cell and bioactive agent immobilization has been the production of very small microbeads so as to minimize the mass-transfer resistance problem associated with large-diameter beads (>1000 μm).

Somatic embryogenesis is a new plant tissue culture technology in which somatic cells (i.e., any cell except a germ or seed cell) are used to produce an embryo (i.e., plant in early state of development) [22]. The technique of somatic embryogenesis in liquid culture, which is believed to be an economical way for future production of artificial seeds, may benefit from cell immobilization technology. Encapsulation may aid in the germination of somatic embryos by allowing for higher cell densities, protecting cells from shear damage in suspension culture,

allowing for surface attachment in the case of anchorage dependent cells, and being very suitable for scale-up in bioreactors.

The long-term objective of the project reported in this section is the development of an economical method for the mass production of artificial seeds using somatic embryogenesis and cell immobilization technology. The short-term aim was to investigate the production of small alginate microbeads using an electrostatic droplet generator. Callus tissue from Carnation leaves was also immobilized and cultured.

4.1 IMMOBILIZED PLANT TISSUE GROWTH

Immobilized callus cells from carnation leaves retained viability as observed by cell growth and plantelet formation [19-21]. In a related study, Shigeta [23] was able to germinate and grow encapsulated somatic embryos of carrot using a 1% sodium alginate solution, as compared to a 2% alginate solution used in the present investigation. The main findings of our experiment, though, indicated that somatic tissue could be electrostatically extruded and aseptically cultured while retaining viability.

Plantlets obtained from 4% alginate beads on agar, originally immobilized at 10 kV, 6 cm distance, were transferred to sterilized potting mixture at two months culture. The plantlets grew well and showed complete leaf and root development by four months [20]. Suspension culture of encapsulated somatic tissue was less successful. Piccioni [24] in a study investigated the growth of plantlets from alginate encapsulated micropropagated buds of M.26 apple rootstocks. He showed that the addition of growth regulators (e.g., indolebutyric acid) to the somatic tissue culture several days prior to the encapsulated, as well as the addition of the same regulators to the encapsulation matrix, improved the production of plantlets in suspension culture from 10% to more than 60%. We can speculate that culturing the Carnation leaf callus tissue in the presence of growth regulators prior and during encapsulation may enhance the production of plantlets from suspension culture.

Electrostatic droplet generation does not appear to have a negative impact on somatic tissue viability since cell growth and plantlet formation was observed. This is in agreement with similar studies reported for insect cells [18] and mammalian cells [25], where it was shown that high electrostatic potentials did not affect cell viability.

In closing, microencapsulation technology is an exciting area to work in. To be able to develop successful and well-understood systems requires close collaboration between scientists with different areas of expertise such as electrical engineering, microbiology, biochemistry, biomaterials and mathematical modelling. Over the next decade we can expect to see many new areas of application of microencapsulated living cell systems such as in the treatment of diseases requiring tissue transplantation, as well as in bioprocess engineering for the production of high value biologicals.

5. References

1. Goosen, M. F. A. (2002). Microencapsulation Methods: Chitosan and Alginate. In: A. Atala and R. P. Lanza, Eds., Methods of Tissue Engineering. Academic Press, San

Diego. Chapter 76, pp 857-874.
2. Inlow, D., D. Harano, and B. Maiorella, (1987). 194th ACS Meeting, Division of Microbial and Chemical Technology, New Orleans, LA. abstract 70.
3. Hink, W.F., (1982). In: E. Kurstak, Ed., Microbial and Viral Pesticides. Marcel Dekker, New York, pp. 493-506.
4. Knudson, D.L., and T.W. Tinsley, (1974). J.Virology, 14, 934-942.
5. Posillico, E.G., (1986). Bio/Technology, 4(2), 114-121.
6. Balachandran, W., and A.G. Bailey, (1982).The Dispersion of Liquids Using Centrifugal and Electrostatic Forces, IEEE Meeting of the Industrial Application Society, 971-980.
7. Fillimore, G.L., and D.C. Van Lokeren, (1982).Multinozzle Drop Generator Which Produces Uniform Break-up of Continuous Jets, IEEE Meeting of the Industrial Society, 991-998.
8. Keshavarz, T., G. Ramsden, P. Phillips, P. Mussenden, and C. Bucke, (1992). Application of Electric Field for Production of Immobilized Biocatalysts, Biotech. Technique, 6, 445-455.
9. Loscertales, I. G., Barrero, A., Guerrero, I., Cortijo, R., Marquez, M., and Ganan-Calvo. A. M., (2002). Micro/Nano Encapsulation via Electrified Coaxial Liquid Jets. Science, 295, 1695-1698.
10. Rayleigh, Lord, (1945).The Theory of Sound, Dover Publications, New York, Volume II, p. 372
11. Rayleigh, Lord, (1882).On the Equilibrium of Liquid Conducting Masses Charged with Electricity, Phil. Mag., 14, 184-188.
12. Bugarski, B., Q. Li, M.F.A. Goosen, D. Poncelet, R. Neufeld and G. Vunjak, (1994). Electrostatic Droplet Generation: Mechanism of Polymer Droplet Formation, AIChEJ., 40(6), 1026-1031.
13. Taylor, G.I., (1966).The Force Exerted by an Electric Field on Long Cylindrical Conductors, Proc. R. Soc. A, 291, 145-155.
14. DeShon, E.W. and R. Carlson, (1968). Electric Field and Model for Electrical Liquid Spraying. J. Colloid Sci. 28, 161-166.
15. Hommel, M., A.M. Sun and M.F.A. Goosen, (1988).Droplet Generation, Canadian Patent 1,241,598.
16. Sample, S.B., and R. Bollini, (1972).Production of Liquid Aerosols by Harmonic Electrical Spraying, J. Colloid. Sci. 14, 185-193.
17. Luckow, V.A., and M.D. Summers, (1987). Bio/Technology, 6(1), 47-55.
18. King, G. A., Daugulis, A. J., Faulkner, P., Bayly, D., and Goosen, M. F. A., (1989). Alginate Concentration: A Key Factor in Growth of Temperature-Sensitive Baculovirus-Infected Insect Cells in Microcapsules. Biotechnol. and Bioeng., 34, 1085-1091.
19. Goosen, M. F. A. (1999). Mass transfer in immobilized cell systems. in: W. M. Kuhtreiber, R. P. Lanza and W. L. Chick (Eds.), Handbook of Cell Encapsulated Technology and Therapeutics. Birhauser and Springer-Verlag (Publ.). Chapter 2. 18-28.
20. Al-Hajry, H. A., S. A., Al-Maskary, L. M., Al-Kharousi, O., El-Mardi, W. H., Shayya, and M. F. A. Goosen. (1999). Encapsulation and Growth of plant Cell Cultures in

Alginate, Biotechnot. Progress. 15(4), 768-774.

21. Goosen, M. F. A., A. S., Al-Ghafri, O., El-Mardi, M. I. J., Al-Belushi, H. A., Al-Hajri, E. S. E., Mahmoud, and E. C. Consolacion, (1997). Electrostatic droplet generation for encapsulation of somatic tissue: Assessment of high voltage power supply. Biotechnology Progress, 13(4):497-502.
22. Teng W. -L. Y.-J, Liu V.-C., Tsai T.-S. Soong (1994). Somatic embryogenesis of carrot in bioreactor culture systems. Hort. Sci. 29 (11), 1349-1352.
23. Shigeta J. (1995). Germination and growth of encapsulated somatic embryos of carrot for mass propagation. Biotechnol. Tech., 10 (9), 771-776.
24. Piccioni, E. (1997). Plantlets from encapsulated micropropagated buds of M.26 apple rootstock. Plant Cell, Tissue and Organ Culture, 47:255-260.
25. Goosen M. F. A., G. M., O'Shea M. M., Gharapetian M. Sun A. (1986). Immobilization of living cells in biocompatible semipermeable microcapsules: Biomedical and potential biochemical engineering applications. In: Chiellini E. Ed., Polymers in Medicine. Plenum Publishing, New York, p 235.
26. Goosen, M. F. A., 1996). Microencapsulation of Living Cells. In: Willaert, R. G., Baron, G. V. and De Backer, L. (Eds), Immobilized Living Cell Systems: Modelling and Experimental Methods. Wiley, Chichester. Chapter 14, 295-322.